Quantum numbers and band topology of nanotubes

2003 J. Phys. A: Math. Gen. 36 5707

(http://iopscience.iop.org/0305-4470/36/21/302)

INSTITUTE OF PHYSICS PUBLISHING JOURNAL OF PHYSICS A: MATHEMATICAL AND GENERAL

J. Phys. A: Math. Gen. **36** (2003) 5707–5717 PII: S0305-4470(03)58579-1

Quantum numbers and band topology of nanotubes

M Damnjanović[1], I Milošević[1], T Vuković[1] and J Maultzsch[2]

[1] Faculty of Physics, University of Belgrade, POB 368, 11001 Belgrade, Serbia
[2] Institut für Festkörper Physik, Technische Universität Berlin, Hardenbergstr. 36, 10623 Berlin, Germany

E-mail: yqoq@afrodita.rcub.bg.ac.yu

Received 20 January 2003, in final form 7 April 2003
Published 13 May 2003
Online at stacks.iop.org/JPhysA/36/5707

Abstract

Nanotubes as well as polymers and quasi-1D subsystems of 3D crystals have line group symmetry. This allows two types of quantum numbers: roto-translational and helical. The roto-translational quantum numbers are linear and total angular (not conserved) momenta, while the helical quantum numbers are helical and complementary angular momenta. Their mutual relations determine some topological properties of energy bands, such as systematic band sticking or van Hove singularities related to parities. The importance of these conclusions is illustrated by the optical absorption in carbon nanotubes: parity may prevent absorption peaks at van Hove singularities.

PACS numbers: 61.50.Ah, 73.61.Wp, 02.20.Bb

1. Introduction

Carbon nanotubes [1] are one of the most prominent quasi-one dimensional crystals which have been extensively investigated both experimentally and theoretically. They are monoperiodic, i.e. they have translational periodicity only in one direction. Thus their symmetry groups are the line groups [2, 3]; in fact, any line group symmetry is reproduced by single- and double-wall carbon nanotubes (SWNT and DWNT, respectively).

The symmetry of a system *a priori* determines many of its physical properties. For example, the translational periodicity of a crystal leads to the band structure with the Bloch eigenstates. Very general topological characteristics of the bands can be derived directly from symmetry such as their degeneracy, systematic band sticking or crossing and van Hove singularities [6]. In this paper we derive those properties for line groups in general with emphasis on carbon nanotubes. Since these properties are based on symmetry only, they refer to both electron and phonon bands. In particular, we show that parities may induce band extrema. Furthermore, the line group symmetry allows two different types of quantum numbers as will be described below. Both types have been used in

the literature for carbon nanotubes [4, 5]; but their physical content and their advantages or disadvantages for specific physical problems have not yet been clearly presented. We give an detailed analysis of their mutual relations and illustrate their usage for carbon nanotubes.

The symmetry operations of carbon nanotubes include screw-axis operations, translations along and rotations around the tube axis (z-axis), which stem from the 2D translations of the graphene lattice (which is rolled up to form the tube). In addition, there are rotation for π around an axis perpendicular to z, and in achiral tubes only, mirror and glide planes [2, 3]. In general, pure translations lead to a linear quasi-momentum quantum number k and pure rotations to an angular quasi-momentum quantum number m. For any line group which, like the SWNT groups, contains a screw axis, however, two types of decomposition of the group lead to two different sets of quantum numbers labelled (k, m) and $(\tilde{k}, \tilde{m})$. These two sets, corresponding to different choices of coordinates in the momenta space, we will call *linear* and *helical* quantum numbers, respectively. The linear quantum number k corresponds to the pure translational subgroup of the line group and the linear number m to rotations including the rotational parts of the screw axis operations. In contrast, in the helical quantum numbers $(\tilde{k}, \tilde{m})$, the screw axis operations are contained in the roto-translational subgroup corresponding to $\tilde{k}$ while $\tilde{m}$ corresponds to only pure rotations.

The linear (k, m) quantum numbers are more commonly used in the literature for carbon nanotubes, although they have some disadvantages especially for chiral tubes which in this description have a rather complicated band structure. Even more important, the linear number m is not a fully conserved quantum number and thus has to be used carefully. Since depending on the particular physical problem either the linear or the helical quantum numbers are more suitable, it may be required to switch from one to the other description.

We present in section 3 the relation between these two descriptions and give a formula for the calculation of the linear from the helical quantum numbers and vice versa, after having introduced in section 2 the structure of the first family line groups. In section 4 we derive the general properties of the nanotube bands from their symmetry, starting with inorganic chiral nanotubes and giving more details for chiral and achiral carbon nanotubes.

2. The first family line group structure

There are 13 infinite families of the line groups [9]. Each of them is characterized by the screw-axis (including the trivial case of pure translations), principal rotational axis and parities. The line groups of the first family are generated by the screw-axis and pure rotations only; no parity is present. Any other line group contains a first family line group as an index-two or index-four subgroup. Therefore, the irreducible representations of all the line groups are constructed by the irreducible representations of the corresponding first family line group (the former can be obtained from the latter by the index-two subgroup induction in one or two steps). In other words, the structure, irreducible representations and quantum numbers are reduced to the first family subgroup. For other groups parities and their quantum numbers have to be added.

Each first family line group $\boldsymbol{L}$ is commutative and non-symmorphic (i.e. in general it contains a screw-axis), with elements combining translations along and rotations around the tube axis. Two structural characteristics of these groups, two types of decompositions, underlie two different sets of quantum numbers labelling the irreducible representations.

The first decomposition (precisely, central extension) is onto the invariant translational (infinite cyclic) subgroup $\boldsymbol{T}(a)$ (translations by multiples of the period a) and the isogonal

rotational group $\boldsymbol{L}/\boldsymbol{T}(a) \cong \boldsymbol{C}_q$. The decomposition parameters q and a, together with an additional integer p, specify the group in the international notation

$$\boldsymbol{L} = \boldsymbol{L}q_p(a) \qquad q = 1, 2, \ldots \quad p = 0, 1, \ldots, q-1. \tag{1}$$

The roto-translational generators, $\ell(1,0) = (I|a)$ and $\ell(0,1) = (C_q|ap/q)$ (Koster–Seitz notation), enable the elements of $\boldsymbol{L}$ to be obtained as

$$\ell(t, j) = \left(C_q^j \middle| \left(\mathrm{Fr}\left[\frac{jp}{q}\right] + t\right) a\right) \qquad j = 0, \ldots, q-1 \quad t = 0, \pm 1, \ldots. \tag{2}$$

For $j = 0$, the elements $\ell(t, 0)$ form the translational subgroup. Since $\ell(0, 1)$ is the finest rotation C_q followed by a fractional translation, the isogonal group is not a subgroup of $\boldsymbol{L}$ unless $p = 0$ (i.e. when $\boldsymbol{L}$ is symmorphic). This decomposition leads to the linear quantum numbers (k, m), where k corresponds to the translational subgroup with the elements $\ell(t, 0)$ and m corresponds to the set with the elements $\ell(0, j)$, which do not form a subgroup; hence m is not fully conserved (unless $p = 0$).

The other decomposition of the first family line groups is the natural factorization into the direct product of two cyclic subgroups: the infinite helical (screw-axis) subgroup $\boldsymbol{T}_q^r(na)$ and the maximal rotational subgroup $\boldsymbol{C}_n$:

$$\boldsymbol{L} = \boldsymbol{T}_q^r(a) \otimes \boldsymbol{C}_n, \qquad \begin{cases} \text{convention (C1)}: & r = 0, 1, \ldots, q/n, \mathrm{GCD}(q/n, r) = 1 \\ \text{convention (C2)}: & r = 0, 1, \ldots, q, \mathrm{GCD}(q, r) = 1. \end{cases} \tag{3}$$

These two cyclic subgroups are generated by $\tilde{\ell}(1,0) = \left(C_q^r \middle| \frac{n}{q}a\right)$ and $\tilde{\ell}(0,1) = C_n = (C_n|0)$ (helical generators), i.e. each element takes the form

$$\tilde{\ell}(z, s) = \left(C_q^r \middle| \frac{n}{q}a\right)^z C_n^s \qquad s = 0, \ldots, n-1 \quad z = 0, \pm 1, \ldots. \tag{4}$$

The corresponding helical quantum numbers $(\tilde{k}, \tilde{m})$ are both fully conserved, since both $\tilde{\ell}(1, 0)$ and $\tilde{\ell}(0, 1)$ form subgroups of the line group.

Some important details concerning this factorization are derived in appendix A. q is a multiple of n, $q = \tilde{q}n$, and the translational period na of the helical subgroup alone is realized by $\tilde{\ell}(q, 0) = (I|na)$. Therefore, na/q is the length of the structural motive, monomer, and the whole system is obtained by successive action of the screw-axis generator on this monomer. In particular, $\tilde{q}$ consecutive monomers build the translational period of length a. The helical parameter r is not uniquely defined: the same line group elements are obtained if any multiple of $\tilde{q}$ is added to r. This ambiguity is resolved by either of two conventions in (3), (C1) or (C2). In the (C1) convention $r = r_0$, while in (C2) l is chosen such that $r = r_0 + lq/n$ is coprime with q.

Of course, the roto-translational generators ℓ may be expressed in terms of the helical ones, $\tilde{\ell}$, and vice versa:

$$\tilde{\ell}(1,0) = \left(C_q^r \middle| \frac{n}{q}a\right) = \ell(r, 0) \qquad \tilde{\ell}(0,1) = C_n = \ell\left(0, \frac{q}{n}\right) \tag{5}$$

$$\ell(1,0) = (I|a) = \tilde{\ell}\left(\frac{q}{n}, -r \pmod n\right) \qquad \ell(0,1) = \left(C_q \middle| \frac{p}{q}a\right) = \tilde{\ell}\left(\frac{p}{n}, n\mathrm{Fr}\left[\frac{1 - r\frac{p}{n}}{q}\right]\right). \tag{6}$$

This is used in appendix B to interrelate the parameters (q, p, a) and (q, r, n, a) of the roto-translational and helical factorizations of the line groups:

$$n = \mathrm{GCD}(q, p) \qquad r_0 = \left(\frac{p}{n}\right)^{\varphi(\frac{q}{n})-1} \pmod{\frac{q}{n}} \qquad \frac{p}{n} = r^{\varphi(\frac{q}{n})-1} \pmod{\frac{q}{n}}. \tag{7}$$

3. Irreducible representations

The described structural properties have been used to obtain the irreducible representations (IRs) of the first family line groups in two different ways [7, 8], and parametrized by two different sets of quantum numbers. First, the roto-translational decomposition results in the quantum numbers of linear and total angular quasi-momenta, k and m. Alternatively, the helical decomposition involves helical and pure rotational quasi momenta, $\tilde{k}$ and $\tilde{m}$. The IRs are given by the corresponding generator representatives

$$ {}_kA_m(\ell(1,0)) = \mathrm{e}^{\mathrm{i}ka} \qquad {}_kA_m(\ell(0,1)) = \mathrm{e}^{\mathrm{i}ka\frac{p}{q}}\mathrm{e}^{\mathrm{i}m\frac{2\pi}{q}} \qquad k \in \left(-\frac{\pi}{a}, \frac{\pi}{a}\right] \quad m \in \left(-\frac{q}{2}, \frac{q}{2}\right] \tag{8} $$

$$ {}_{\tilde{k}}A_{\tilde{m}}(\tilde{\ell}(1,0)) = \mathrm{e}^{\mathrm{i}\tilde{k}\frac{a}{\tilde{q}}} \qquad {}_{\tilde{k}}A_{\tilde{m}}(\tilde{\ell}(0,1)) = \mathrm{e}^{\mathrm{i}\tilde{m}\frac{2\pi}{n}} \qquad \tilde{k} \in \left(-\tilde{q}\frac{\pi}{a}, \tilde{q}\frac{\pi}{a}\right] \quad \tilde{m} \in \left(-\frac{n}{2}, \frac{n}{2}\right]. \tag{9} $$

The intervals giving the ranges of k and $\tilde{k}$ are called Brillouin zones; m and $\tilde{m}$ take only integer values from the intervals above. It is assumed that all the equalities in k and m are modulo these intervals. From (8) and (9) follows:

$$ {}_kA_m(\tilde{\ell}(1,0)) = \mathrm{e}^{\mathrm{i}k\frac{a}{\tilde{q}}}\mathrm{e}^{\mathrm{i}mr\frac{2\pi}{q}} \qquad {}_kA_m(\tilde{\ell}(0,1)) = \mathrm{e}^{\mathrm{i}m\frac{2\pi}{n}} \tag{10} $$

$$ {}_{\tilde{k}}A_{\tilde{m}}(\ell(1,0)) = \mathrm{e}^{-\mathrm{i}\tilde{m}r\frac{2\pi}{n}}\mathrm{e}^{\mathrm{i}\tilde{k}a} \qquad {}_{\tilde{k}}A_{\tilde{m}}(\ell(0,1)) = \mathrm{e}^{\mathrm{i}\tilde{m}\frac{1-r\frac{p}{q}}{\tilde{q}}\frac{2\pi}{n}}\mathrm{e}^{\mathrm{i}\tilde{k}a\frac{p}{q}}. \tag{11} $$

Since the $\tilde{k}\tilde{m}$-numbers are independently defined on the different generators, the same representation is obtained for any $\tilde{m}' = \tilde{m} + \tilde{M}n$ and/or $\tilde{k}' = \tilde{k} + \tilde{K}\tilde{q}2\pi/a$. Nevertheless, from (10) it follows that ${}_kA_m = {}_{k'}A_{m'}$ if and only if simultaneously $m' = m + Mn$ and $k' = k + K2\pi/a$ such that $Mr = -K \pmod{\tilde{q}}$; due to $r\frac{p}{n} = 1 \pmod{\tilde{q}}$, this allows simultaneous changes $k' = k + K2\pi/a$ and $m' = m - pK \pmod{q}$.

Each irreducible representation of $\boldsymbol{L}$ is labelled by both sets of quantum numbers, (k, m) and $(\tilde{k}, \tilde{m})$. The equality ${}_{\tilde{k}}A_{\tilde{m}}(\ell) = {}_kA_m(\ell)$ for each $\ell \in \boldsymbol{L}$ establishes the correspondence between the pairs $(\tilde{k}, \tilde{m})$ and (k, m). The transition rules $(k, m) \to (\tilde{k}, \tilde{m})$ are obtained by comparison of (10) and (9):

$$ (k, m) \to (\tilde{k}(k, m), \tilde{m}(m)) = \left(k + \frac{rm}{n}\frac{2\pi}{a} + \tilde{K}\tilde{q}\frac{2\pi}{a}, m + \tilde{M}n\right) \tag{12} $$

the integers $\tilde{K}$ and $\tilde{M}$ are uniquely (and independently) determined by the requirement that $\tilde{k}$ and $\tilde{m}$ are from the intervals given in (9). Analogously, from (8) and (11) it follows:

$$ (\tilde{k}, \tilde{m}) \to (k(\tilde{k}, \tilde{m}), m(\tilde{k}, \tilde{m})) = \left(\tilde{k} - \tilde{m}\frac{r}{n}\frac{2\pi}{a} + K\frac{2\pi}{a}, \tilde{m} - Kp + Mq\right) \tag{13} $$

where K and M are again integers used to get the momenta from the intervals given by (8). Note that now K must be found first because M depends on K.

Together with the helical quantum number $\tilde{k}$, labelling the representations (9), the transition rules depend on the r-convention. Indeed, the choice of r determines the helicity of the momentum $\tilde{k}$: the unit change of the total momentum m leads to the same change of $\tilde{m}$ (assuming $n > 1$) and a simultaneous change of $\tilde{k}$ for $2r\pi/na$. Analogously, a change of the helical momentum by $2\pi/a$ preserves the linear momentum k and induces a jump by p of the total angular momentum m.

For the different allowed k and fixed m one gets the m-series, or the m-band, over the Brillouin zone $k \in (-\pi/a, \pi/a]$ of the representations. Analogously, the $\tilde{m}$-bands are defined over the helical Brillouin zone $\tilde{k} \in (-\pi\tilde{q}/a, \pi\tilde{q}/a]$. From (12) it follows that the whole set

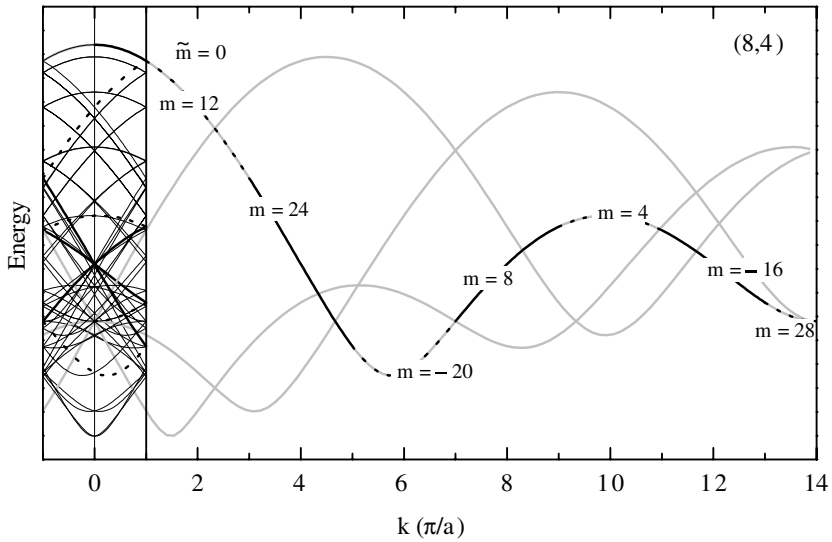

Figure 1. Conduction bands of the (8, 4) carbon nanotube calculated within the first-neighbour tight binding approximation [8]. In the left panel, the bands are shown in the linear (k, m) description; on the right the bands are given by the helical $(\tilde{k}, \tilde{m})$ quantum numbers. In the (8, 4) tube, $q = 56$, $n = 4$, $\tilde{q} = 14$ and $p = 44$. Thus there are 56 (k, m) bands with $k \in (-\pi/a, \pi/a]$ or 4 $(\tilde{k}, \tilde{m})$ bands with $\tilde{k} \in (-14\pi/a, 14\pi/a]$. The bold solid and dotted lines represent those linear m bands, which, being unfolded, yield the helical band $\tilde{m} = 0$. The band indices are given in the figure.

of $\tilde{q}$ different m-bands with m differing by multiples of n gives exactly a single $\tilde{m}$-band with $\tilde{m} = m \pmod n$. Since $\tilde{k}(k, m) + 2\pi/a = \tilde{k}(k, m + \tilde{p} \pmod q)$, the segment of the helical Brillouin zone of the $\tilde{m}$-band corresponding to the m-band (thus $m = \tilde{m} + Mn$ for some M) is followed by the segment corresponding to $(m + p \pmod q)$ band; these $\tilde{q}$ different segments continuously fill up the $\tilde{m}$-band. This is illustrated in figure 1, where we show the conduction bands of the (8, 4) carbon nanotube given by both linear (k, m) and helical $(\tilde{k}, \tilde{m})$ quantum numbers. The $\tilde{m}$-bands can be thought of as consisting of the 'unfolded' m-bands. There are $n = 4$ $\tilde{m}$-bands with $\tilde{k} \in (-14\pi/a, 14\pi/a]$ and $q = 56$ m-bands with $k \in (-\pi/a, \pi/a]$. Thus in the description by the helical quantum numbers $(\tilde{k}, \tilde{m})$, the number of bands is smaller by a factor of $\tilde{q} = 14$ than for the linear quantum numbers, but the range of $\tilde{k}$ is increased by the same factor.

The physical contents of the obtained quantum numbers are seen from the irreducible representations. From the first of equations (8) it follows that k is canonically conjugated to the discrete translations, i.e. k is the conserved linear quasi-momentum. Further, in the second equation (8) the same ratio p/q both in the generator and in the exponent means that k is completely related to the fractional translation of $\ell(0, 1)$. Then the remaining m-dependent part appears due to the isogonal rotation C_q, and m is the corresponding angular momentum (component along the rotational axis of C_q). Unless $\boldsymbol{L}$ is symmorphic, C_q is not its element, and m is not a conserved quantum number. As for the $\tilde{k}\tilde{m}$-numbers, from the first equation of (9) it follows that $\tilde{k}$ combines angular and linear momenta into the helical momentum conjugated to the helix chosen by the r-convention. The complementing helical momentum $\tilde{m}$ is the angular momentum related to the pure rotations of the point subgroup $\boldsymbol{C}_n$. Both

Table 1. Analysis of the representations ($\tilde{k} = 0, \tilde{q}\pi/a, \tilde{m} = 0, n/2$). The last four columns give their km quantum numbers depending on the parities of $\tilde{q}$, A and $\tilde{p}$ (defined by $\tilde{p}r = 1 + A\tilde{q}$). Being coprimes, $\tilde{q}$ and $\tilde{p}$ cannot be simultaneously even; when $\tilde{q}$ is odd, A and $\tilde{p}$ are of opposite parity. Since $\tilde{m} = n/2$ only when n is even, then both p and q are even, and in the convention (C2) r is odd (column 4). For the symmorphic groups $q = n$, $p = \tilde{p} = 0$ and $\tilde{q} = 1$. When $q = 2p$, then $p = n$, $\tilde{q} = 2$, $\tilde{p} = 1$, $A = 0$ (column 2). For nanotubes with hexagonal lattice, $\tilde{q} = 2 \pmod{12}$ (columns 1, 2).

	(k, m)			
	$\tilde{q}$ even		$\tilde{q}$ odd	
$(\tilde{k}, \tilde{m})$	A even	A odd	$\tilde{p}$ even	$\tilde{p}$ odd
$(0, 0)$	$(0, 0)$	$(0, 0)$	$(0, 0)$	$(0, 0)$
$(0, \frac{n}{2})$	$(\frac{\pi}{a}, -\frac{p}{2})$	$(\frac{\pi}{a}, \frac{q-p}{2})$	$(\frac{\pi}{a}, \frac{q-p}{2})$	$(\frac{\pi}{a}, -\frac{p}{2})$
$(\tilde{q}\frac{\pi}{a}, 0)$	$(0, \frac{q}{2})$	$(0, \frac{q}{2})$	$(\frac{\pi}{a}, -\frac{p}{2})$	$(\frac{\pi}{a}, \frac{q-p}{2})$
$(\tilde{q}\frac{\pi}{a}, \frac{n}{2})$	$(\frac{\pi}{a}, \frac{q-p}{2})$	$(\frac{\pi}{a}, -\frac{p}{2})$	$(0, \frac{q}{2})$	$(0, \frac{q}{2})$

quantum numbers $\tilde{k}$ and $\tilde{m}$ are conserved. The inherent physical meaning of the quantum numbers makes one or the other choice more suitable for different physical considerations.

For example, we consider optical transitions in carbon nanotubes. They are almost vertical in the linear Brillouin zone, i.e. $\Delta k = 0$. Thus no crossing of the Brillouin zone edge occurs, where bands with different m meet, and m can be treated as a conserved quantum number. On the other hand, if an electron is scattered by, e.g., a phonon, the linear quasi-momentum k changes and possibly crosses the Brillouin zone edge. In this case, m is no longer conserved and the $(\tilde{k}, \tilde{m})$ numbers are more suitable.

The special points in the one-dimensional Brillouin zone are its centre and the edge. The real representations with $\tilde{k} = 0, \tilde{q}\pi/a$ and $\tilde{m} = 0$ and (if n is even only) $\tilde{m} = n/2$ are particularly important: these are either the identity representation (${}_{\tilde{k}=0}A_{\tilde{m}=0}(\ell) = 1$ for all the elements of $\boldsymbol{L}$) or alternating representations (half of the elements are represented by 1 and the other half by -1). The (k, m) quantum numbers of these representations may be found by the transition rules, and the analysis is presented in table 1.

In addition to the symmetry operations of first family line groups, carbon nanotubes contain a two-fold rotational axis (U axis) perpendicular to the tube axis and, achiral tubes only, mirror and glide planes. In general, if the first family line groups are enlarged by the U axis the fifth family groups are obtained. The special cases of the groups with $q = n$ (symmorphic) and $q = 2n$ allow the incorporation also of mirror, glide and roto-reflection planes yielding the remaining 11 families. Therefore, the previous results should be specified for these groups. As for the symmorphic groups $\boldsymbol{L} = \boldsymbol{T}_n^1\boldsymbol{C}_n = \boldsymbol{L}n_0$, both decompositions and corresponding generators coincide; thus $\tilde{k} = k$ and $\tilde{m} = m$, leaving only one type of representation. In the case $q = 2n$, one has $\tilde{q} = 2, r = 1$ (in both conventions) and $p = n$: $\boldsymbol{L} = \boldsymbol{T}_{2n}^1\boldsymbol{C}_n = \boldsymbol{L}2n_n$. The transition rules between the generators are easily found from (5) and (6):

$$\tilde{\ell}(1, 0) = \ell(2, 0) \qquad \ell(0, 1) = \tilde{\ell}(1, 0) \qquad \tilde{\ell}(0, 1) = \ell(-1, 2). \tag{14}$$

The irreducible representations and their transition rules follow directly from (8)–(10) and (12), (13).

4. Band assignation and degeneracy

The high and diverse symmetry of nanotubes makes group theoretical techniques extraordinarily fruitful in their studies [2, 6]. In general, the symmetry group of single-wall

inorganic nanotubes [3] is from the first family; the additional vertical and horizontal mirror planes for the special achiral (zig-zag and armchair) chiralities give the fourth and eighth families, respectively. Only single-wall carbon nanotubes, built solely of carbon atoms, have in addition the U-axis symmetry. Thus, the line group of chiral SWNTs is from the fifth family, while for both achiral types, zig-zag and armchair tubes, the thirteenth family is obtained. Both sets of roto-translational (k, m) or helical $(\tilde{k}, \tilde{m})$ quantum numbers, described in the previous section, are used in studies of nanotubes [4, 5].

In the simplest case of inorganic chiral tubes, when the symmetry group is from the first family, the eigen problem $H|x\rangle = E|x\rangle$ of the Hamiltonian H of a subsystem (e.g., electron or phonon subsystem) is solved by the Bloch functions $|km; \lambda\rangle$ or generalized Bloch functions $|\tilde{k}\tilde{m}; \lambda\rangle$. Here λ counts different states with the same quantum numbers. The Bloch function $|km; \lambda\rangle$ describes a quantum state of a (quasi)particle propagating along the tube axis with the quasi-momentum k and the z-component of the angular momentum m; analogously, $|\tilde{k}\tilde{m}; \lambda\rangle$ is a state with sharp helical and complementary angular momenta. For fixed m (or $\tilde{m}$) and λ the corresponding eigen energies $\epsilon_m^\lambda(k)$ and $\epsilon_{\tilde{m}}^\lambda(\tilde{k})$ continuously depend on k (or $\tilde{k}$). Thus, to a band of the representations in general correspond several energy bands, differing in λ. It should be emphasized that the electron or phonon Hamiltonians, which are usually considered, commute with time reversal. Exactly like the U-axis, this operation reverses all the involved momenta. Based on the irreducible co-representations instead of the representations in the SWNT case, the further discussion is essentially the same as for SWNT energy bands. This also means that time reversal gives no further degeneracy for SWNTs.

The fifth family symmetry group of a chiral SWNT contains in addition the U-axis, i.e. a rotation by π about an horizontal axis. The same two sets of quantum numbers parametrize the irreducible representations [8, 11]. Since the U axis reverses all the momenta, it maps $|\tilde{k}, \tilde{m}\rangle$ to $|-\tilde{k}, -\tilde{m}\rangle$, and vice versa. As far as these two states are different, the corresponding energy levels are degenerate: labels λ may be chosen such that

$$\epsilon_{\tilde{m}}(\tilde{k}) = \epsilon_{-\tilde{m}}(-\tilde{k}) = \epsilon_{-\tilde{m}}(2\tilde{q}\pi/a - \tilde{k}) \tag{15}$$

$$\epsilon_{\tilde{m}}(\tilde{q}\pi/a - \tilde{k}) = \epsilon_{-\tilde{m}}(\tilde{q}\pi/a + \tilde{k}). \tag{16}$$

The doublet of states $|\tilde{k}, \tilde{m}\rangle$ and $|-\tilde{k}, -\tilde{m}\rangle$ spans the two-dimensional space carrying the irreducible representation ${}_{\tilde{k}}E_{\tilde{m}}$ with integer $\tilde{m} \in (-n/2, n/2]$. Therefore, it suffices to consider $\tilde{k}$ in the interval $[0, \tilde{q}\pi/a]$ being the irreducible domain [12]. Only if simultaneously $k = 0, \tilde{q}\pi/a$ and $m = 0, n/2$, the states $|\tilde{k}, \tilde{m}\rangle$ and $|-\tilde{k}, -\tilde{m}\rangle$ are physically the same: $|-\tilde{k}, -\tilde{m}\rangle = \pm|\tilde{k}\tilde{m}\rangle$. Thus, at the edges of the irreducible domain even and odd states appear: $|00\pm\rangle$, $|\tilde{q}\pi/a, 0\pm\rangle$, and, only for n even, $|0, n/2, \pm\rangle$ and $|\tilde{q}\pi/a, n/2, \pm\rangle$. These singlet states correspond to the one-dimensional representations ${}_0A_0^\pm$, ${}_{\tilde{q}\pi/a}A_0^\pm$, ${}_0A_{n/2}^\pm$ and ${}_{\tilde{q}\pi/a}A_{n/2}^\pm$. All other states are doublets, yielding at least double-degenerate energy bands over the interior of the irreducible domain. Those with opposite $\tilde{m}$ meet at $\tilde{k} = 0, \tilde{q}\pi/a$. Only for the bands $\tilde{m} = 0, n/2$, when $-\tilde{m} = \tilde{m}$, equations (15) and (16) become

$$\epsilon_{\tilde{m}}(\tilde{k}) = \epsilon_{\tilde{m}}(-\tilde{k}) \qquad \epsilon_{\tilde{m}}(\tilde{q}\pi/a - \tilde{k}) = \epsilon_{\tilde{m}}(\tilde{q}\pi/a + \tilde{k}). \tag{17}$$

Thus these bands are symmetric around $\tilde{k} = 0$ and $\tilde{q}\pi/a$, respectively. Therefore, they must have extrema (i.e. peaks in the density of states) at $\tilde{k} = 0$ and $\tilde{k} = \tilde{q}\pi/a$, where they end by even or odd singlet states. In fact, these singularities are essentially a consequence of the U-axis parity.

Also with the (k, m)-numbers, the Bloch states $|km\rangle$ and $|-k, -m\rangle$ form a degenerate doublet, corresponding to the two-dimensional irreducible representation ${}_kE_m$. Again, the energy bands (as well as the representation bands) are defined over the irreducible domain

$k \in [0, \pi/a]$, while m takes on the same values as in (8). Analogously to the representation bands, each energy $\tilde{m}$-band contains $\tilde{q}$ energy m-bands with $m = \tilde{m} + in$ $(i = 0, \ldots, \tilde{q})$. The part of the $\tilde{m}$-band corresponding to m is followed by the part corresponding to $m + p$ (mod q). The systematic band sticking at the Brillouin zone edges is given by the U-axis operation and follows from (15) (at $k = 0$), and (16) and (13) at $k = \pi/a$ (see also figure 1):

$$\epsilon_m(k) = \epsilon_{-m}(-k) \qquad \epsilon_m(\pi/a - k) = \epsilon_{m+p} \,(\mathrm{mod}\, q\,(\pi/a + k). \tag{18}$$

Although $k = 0$ is invariant under U, for $m = 1, \ldots, q/2 - 1$, the states $|0m\rangle$ and $|0, -m\rangle$ are again a two-dimensional doublet of the irreducible representations ${}_0E_m$. Only the states corresponding to $\tilde{k} = 0, \tilde{q}\pi/a$ and $\tilde{m} = 0, n/2$ are singlets (see table 1). At the U-invariant edge $k = 0$, the one-dimensional irreducible representations ${}_0A_0^{\pm}$ and ${}_0A_{q/2}^{\pm}$ are carried by either even or odd states $|0, m = 0\pm\rangle$ and $|0, m = q/2, \pm\rangle$. Analogously, $k = \pi/a$ is mapped by the U-axis operation to $k = -\pi/a$, which is equivalent to the irreducible Brillouin zone point π/a. Thus, π/a is U-invariant, but according to (13) m is changed to $m' = -p - m$, and U intertwines the states $|\pi/a, m\rangle$ and $|\pi/a, m'\rangle$. The singlets $|\pi/a, -p/2, \pm\rangle$ and $|\pi/a, (q - p)/2, \pm\rangle$ appear only for p even and correspond to the one-dimensional representations ${}_{\pi/a}A_{-p/2}^{\pm}$ and ${}_{\pi/a}A_{(q-p)/2}^{\pm}$. The remaining integers $m \in (-p/2, (q - p)/2)$ give the double-degenerate levels of the representations ${}_{\pi/a}E_m$. The bands with m and m' differ in the interior of the irreducible domain, but they stick together at $k = \pi/a$ as well as those with m and $-m$ stick together at $k = 0$. The exceptions are the bands $m = 0, \frac{q}{2}$ at $k = 0$ and $m = -\frac{p}{2}, \frac{q-p}{2}$ at $k = \pi/a$:

$$\epsilon_m(k) = \epsilon_m(-k) \qquad \epsilon_m(\pi/a - k) = \epsilon_m(\pi/a + k). \tag{19}$$

Again, it follows that the singlet states at the edges are van Hove singularities of the corresponding bands.

The mirror planes, σ_v and $\sigma_\mathrm{h} = U\sigma_\mathrm{v}$, yield new parities in the cases of zig-zag ($\mathcal{Z}$) and armchair ($\mathcal{A}$) tubes. Even and odd states with respect to σ_v are labelled by A and B. The parity of the horizontal mirror plane σ_h is denoted as that of U, i.e. '+'; and '−' now points to the even and odd states with respect to either one of these z-reversing operations. Obviously, σ_v leaves k invariant while m is reversed, forcing m and $-m$ bands to coincide. This causes additional degeneracy. Therefore, in the interior of the irreducible domain, the U-degenerate states $|km\rangle$ and $|-k, -m\rangle$ are mapped by σ_v onto $|k, -m\rangle$ and $|-k, m\rangle$. For each $m = 1, \ldots, n - 1$ all these states span the four-dimensional irreducible representation ${}_kG_m$ of the four-fold degenerate band. Only for $m = 0, n$ does the degeneracy remain two-fold, in accordance with the two-dimensional irreducible representations ${}_kE_0^{A/B}$ and ${}_kE_n^{A/B}$ over σ_v-even or odd states $|km, A/B\rangle$ and $|-km, A/B\rangle$. If further $k = 0$, the states $|00, \pm, A/B\rangle$ and $|0n, \pm, A/B\rangle$ are non-degenerate, corresponding to the one-dimensional representations ${}_0A_0^{\pm}$, ${}_0B_0^{\pm}$, ${}_0A_n^{\pm}$ and ${}_0B_n^{\pm}$. For the remaining $m = 1, \ldots, n - 1$, the states $|0m\pm\rangle$ and $|0, -m\pm\rangle$ are degenerate giving two-dimensional representations ${}_0E_m^{\pm}$ (parity with respect to σ_h). At the other edge $k = \pi/a$, for integer $m \in (0, n/2)$ the four-fold degenerate states $|\pi/a, m\rangle$, $|\pi/a, -m\rangle$, $|\pi/a, n - m\rangle$ and $|\pi/a, m - n\rangle$ span the representation ${}_{\pi/a}G_m$. As for $m = 0, n$, the states $|\pi/a, 0, A/B\rangle$ and $|\pi/a, n, A/B\rangle$ as well as the states (existing only for n even) $|\pi/a, n/2, \pm\rangle$ and $|\pi/a, -n/2, \pm\rangle$ are degenerate, being associated with the representations ${}_{\pi/a}E_0^{A/B}$ and ${}_{\pi/a}E_{n/2}^{\pm}$. Due to mirror symmetry, the first equality (19) for each m and $k = 0$ is fulfilled, as well as the second one for $m = n/2$ (at π/a). Thus, the z-reversal parity again characterizes all the states at the edges of the bands satisfying (19), and therefore coincides with van Hove singularities; this includes all bands at $k = 0$ and the $m = n/2$ band (only if n even) at $k = \pi/a$.

We conclude that the systematic band degeneracy is caused by the parities and/or time reversal. Their nontrivial action on the momenta eigenstates defines the irreducible

representations of the symmetry group with dimension 2 (E) or 4 (G); only for some particular values of the momenta is the action trivial giving non-degenerate representations A and B. The representations uniquely correspond to each complete set of quantum numbers (momenta and parities).

5. Discussion

A number of the symmetry-based characteristics of the energy bands of nanotubes has been derived. These properties refer to any (quasi)particle subsystem bands, in particular to the electron and phonon bands.

Two structural characteristics of the line groups allow the nanotube band assignment by either helical [5] or roto-translational [4] quantum numbers. Based on the factorization onto subgroups, the helical quantum numbers are the conserved helical $\tilde{k}$ and remaining angular momentum $\tilde{m}$. They give simple insight into the band topology. The roto-translational quantum numbers reflect the symmetry group decomposition onto the translational subgroup (conserved linear momentum k) and the isogonal factor group (nonconserved angular momentum m). Since this structure is the same for 3D crystals, the consequent linear and total angular momentum are more customary, although the latter are not conserved. The rules of transitions from one to the other set of quantum numbers facilitate the analysis of the band topology in terms of (k, m)-numbers. These two sets coincide if and only if the symmetry group is symmorphic.

Due to the time reversal symmetry, which like the U axis reverses all momenta, the symmetry-based properties of the bands of any single-wall nanotube are the same as for the carbon ones. Thus, instead of the Brillouin zone, only its nonnegative half (irreducible domain) completely determines the bands. The systematic band degeneracy is two-fold for chiral tubes; for the achiral ones it is four-fold, besides double degenerate bands with odd or even vertical mirror parity. At the edges of the Brillouin zone less degenerate states may occur with odd and even z-reversal parity.

Each $\tilde{m}$-band consists of $\tilde{q}$ m-bands which pairwise meet at the Brillouin zone edges. Since $\tilde{q} = 2 \pmod{12}$, being two for achiral tubes, it appears that the m-bands of the achiral tubes are grouped in pairs meeting at π/a. But the band structure of a chiral tube contains large groups of $\tilde{q} = 14, 26, \ldots$ bands with $m = \tilde{m} + in$ connected at $k = 0, \pi/a$.

Finally, symmetry implies some of the van Hove singularities. These singularities coincide with the z-reversal parity (U-axis or horizontal mirror plane) odd and even states. Thus, for chiral tubes, among $q = 14n, 26n, \ldots$ types of bands, only four at $k = 0$ and (for even n) at $k = \pi/a$ are even or odd. In contrast, every achiral band has a van Hove singularity at $k = 0$; for even n, the $m = n/2$-bands are singular at $k = \pi/a$ as well.

The importance of the coincidental z-reversal parity and van Hove singularities is nicely illustrated by the optical transitions in zig-zag tubes. For the incoming light with polarization orthogonal to the tube axis, the selection rules for absorption are

$$\Delta k = 0 \quad \text{(vertical transition)} \qquad \Delta m = \pm 1. \tag{20}$$

The density of states has a peak at $k = 0$, apparently suggesting an absorption peak at the energies corresponding to the transitions. Nevertheless, at $k = 0$ the parities of the bands with $\Delta m = \pm 1$ are opposite; since for the considered polarization the incoming light has even horizontal mirror parity, the transitions are actually forbidden. Thus, the frequently used JDOS approximation (including only the selection rules (20)) is inappropriate. Of course, besides these systematic extrema caused by z-reversal parities, others may appear [13] depending on the considered model.

Appendix A. Properties of the helical groups

For any two positive integers Q and R and each positive real f, the transformation $\left(C_Q^R|f\right)$ generates the infinite cyclic group of the screw-axis:

$$\boldsymbol{T}_Q^R[f] = \left\{\left(C_Q^R|f\right)^z = \left(C_Q^{Rz}|fz\right)|z = 0, \pm 1, \ldots\right\}.$$

The notation is non-unique: different choices of Q and R may give the same group. Since $C_Q^R = C_Q^{R'=R \pmod Q} = C_{Q/\mathrm{GCD}(R',Q)}^{R'/\mathrm{GCD}(R',Q)}$, this ambiguity is fixed by the condition that R is positive, less than Q and coprime with Q. Then the minimal pure translation is $\left(C_Q^R|f\right)^Q = (I|Qf)$, i.e. the translational period of the screw-axis group is $A = Qf$. Finally, the standard notation for the generator $\left(C_Q^R\left|\frac{A}{Q}\right.\right)$ and group are

$$\boldsymbol{T}_Q^R(A) = \left\{\left(C_Q^R\left|\frac{A}{Q}\right.\right)^z\right\} \qquad Q = 1, 2, \ldots \qquad 0 \leqslant R < Q \quad \mathrm{GCD}(Q, R) = 1. \tag{A.1}$$

The pure translational group is obtained for $R = 0$; then $Q = 1$ by convention.

For each Q, R, $n = 1, 2, \ldots$ the elements of the groups $\boldsymbol{T}_Q^R(A)$ and $\boldsymbol{C}_n$ commute, enabling the construction of their direct product, being obviously the first family line group. Now, $\boldsymbol{C}_n$ introduces an additional non-uniqueness (besides the resolved one in R): pure rotations of the total group are contained in $\boldsymbol{C}_n$ (thus n is unique), but n different screw-axis groups, generated by $\left(C_Q^R C_n^s\left|A/Q\right.\right)$ for $s = 0, \ldots, n-1$, can equally well be used to obtain the same line group. The fractional translations of all these generators are the same, as well as the minimal isogonal rotation, and its order is $q = nQ/\mathrm{GCD}(n, Q)$. Thus, a new standardization resolving this non-uniqueness is the choice of a helix. To get it, we first rewrite all helical generators in the form $\left(C_q^{Rn/\mathrm{GCD}(n,Q)+s\tilde{q}}\left|A/Q\right.\right) = \left(C_q^{r_l}\left|A/Q\right.\right)$ $(l = 0, \ldots, n-1)$, with $r_0 = Rn/\mathrm{GCD}(n, Q) \pmod{\tilde{q}}$ and $r_l = r_0 + l\tilde{q}$. All products $\boldsymbol{T}_q^{r_l}(A) \otimes \boldsymbol{C}_n$ are the same group $\boldsymbol{L}$. Obviously, r_0 is coprime with $\tilde{q}$ (since R is coprime with q) and singles out the generator with minimal rotation, producing therefore the most slanted helix. By one convention, denoted by (C1), r_0 is chosen for r. Another one, (C2), is to use the minimal r_l being coprime with q. The translational period a of $\boldsymbol{L}$ is obtained from the relation $(I|a) = \left(C_q^{rz}\left|zA/q\right.\right)C_n^s$; using $\mathrm{GCD}(r, \tilde{q}) = 1$, it is solved by $z = i\tilde{q}$, and the minimal solution (for $i = 1$) gives $a = A/n$. Summarizing, the first family line group $\boldsymbol{L}$ in the factorized form (3) is uniquely given by positive integers q, r, n and positive real a.

Appendix B. Relations between the helical and the roto-translational notation

Among the $\boldsymbol{L}$ elements $\ell(t, j) = \left(C_q^j\left|(\mathrm{Fr}[jp/q]+t)a\right.\right)$, pure rotations $C_n^s = \tilde{\ell}(0, s)$ are singled out by vanishing of the translational part, $\mathrm{Fr}[jp/q]+t = 0$. This gives two independent requirements: the integer part implies $t = 0$, while the fractional translation $\mathrm{Fr}[jp/q] = 0$ if and only if $j = sq/\mathrm{GCD}(q, p)$. This gives $C_n^s = C_q^{sq/\mathrm{GCD}(q,p)} = C_{\mathrm{GCD}(q,p)}^s$, implying further $n = \mathrm{GCD}(q, p)$ and $\tilde{\ell}(0, s) = \ell(0, s\tilde{q})$.

The fractional translation of the helical generator is only $a/\tilde{q}$. Thus, $t = 0$ in the equation $\tilde{\ell}(1, 0) = \ell(t, j)$ simplifying to $\left(C_q^r\left|a/\tilde{q}\right.\right) = \left(C_q^j\left|\mathrm{Fr}[j\tilde{p}/\tilde{q}]a\right.\right)$ (here $\tilde{p} = p/n$). The equality of the translational parts yields the condition $\mathrm{Fr}[j\tilde{p}/\tilde{q}] = 1/\tilde{q}$ for j, i.e. $j\tilde{p} = 1 \pmod{\tilde{q}}$. The reduced system of roots is just the set of possible (equivalent) values r_l of r, with one solution given in terms of Euler's function φ (Euler's theorem is applicable since $\mathrm{GCD}(\tilde{p}, \tilde{q}) = 1$): the inverse if $\tilde{p}$ modulo $\tilde{q}$ is $j = r_0 = \tilde{p}^{\varphi(\tilde{q})-1} \pmod{\tilde{q}}$. Obviously, $\mathrm{GCD}(r_0, \tilde{q}) = 1$ and $r_0 < \tilde{q}$, thus this minimal value is r for the convention (C1). Also, this means that $\tilde{p}$ is the inverse of r (in both conventions) modulo $\tilde{q}$.

All this is used to derive the interrelations (5) and (6) of two sets of the generators. In the last one it should be noted that $s = (1 - r\tilde{p})/\tilde{q} \pmod{n} = n\mathrm{Fr}[(1 - r\tilde{p})/q]$, since $r\tilde{p} = 1 \pmod{\tilde{q}}$ is the solution of $s\tilde{q} + r\tilde{p} = 1 \pmod{q}$.

References

[1] Iijima S 1991 *Nature* **354** 56
[2] Damnjanović M, Milošević I, Vuković T and Sredanović R 1999 *Phys. Rev.* B **60** 2728–39
[3] Milosević I , Damnjanović M, Vuković T and Nikolić B 2000 *Eur. Phys. J.* B **17** 707–12
[4] Hamada N, Sawada S and Oshiyama A 1992 *Phys. Rev. Lett.* **68** 1579
Dresselhaus M S, Dresselhaus G and Eklund P C 1998 *Science of Fullerenes and Carbon Nanotubes* (San Diego, CA: Academic)
Saito R, Dresselhaus G and Dresselhaus M 1998 *Physical Properties of Carbon Nanotubes* (London: Imperial College Press)
[5] White T C, Robertson D H and Mintmire J W 1993 *Phys. Rev.* B **47** 5485
Jishi R A, Venkataraman L, Dresselhaus M S and Dresselhaus G 1995 *Phys. Rev.* B **16** 11176
White C T and Todorov T N 1998 *Nature* **323** 240
Tasaki S, Maekawa K and Yamabe T 1998 *Phys. Rev.* B **57** 9301
[6] Vuković T, Milošević I and Damnjanović M 2002 *Phys. Rev.* B **65** 045418
[7] Bozovic I, Vujicic M and Herbut F 1978 *J. Phys. A: Math. Gen.* **11** 2133
Bozovic I and Vujicic M 1981 *J. Phys. A: Math. Gen.* **14** 777
[8] Milošević I and Damnjanović M 1993 *Phys. Rev.* B **47** 7805–18
Damnjanović M, Vuković T and Milošević I 2000 *J. Phys A: Math. Gen.* **33** 6561–72
[9] Vujicic M, Bozovic I and Herbut F 1977 *J. Phys. A: Math. Gen.* **10** 1271
[10] Lin-Chung P J and Rajagopal A K 1994 *J. Phys: Condens. Matter* **6** 3697–706
[11] Kirschner I and Meszaros Cs 2001 *J. Phys.: Condens. Matter* **13** 5399–411
[12] Altmann S L 1991 *Band Theory of Solids. An Introduction from the Point of View of Symmetry* (Oxford: Clarendon)
Altmann S L 1977 *Induced Representations in Crystals and Molecules* (London: Academic)
[13] Reich S and Thomsen C 2000 *Phys. Rev.* B **62** 4273